ACS APPLIED MATERIALS & INTERFACES

Research Article

www.acsami.org

Improved SERS Nanoparticles for Direct Detection of Circulating Tumor Cells in the Blood

Xiaoxia Wu,[†,‡] Liqiang Luo,[†] Sugeun Yang,[§] Xuehua Ma,[‡] Yonglong Li,[‡] Chen Dong,[‡] Yuchen Tian,[‡] Ling'e Zhang,[‡] Zheyu Shen,*[,‡] and Aiguo Wu*[,‡]

[†]College of Sciences, Shanghai University, 99 Shangda Road, Shanghai 200444, China

[‡]Division of Functional Materials and Nano Devices, Ningbo Institute of Materials Technology & Engineering, & Key Laboratory of Magnetic Materials and Devices, Chinese Academy of Sciences, Ningbo, Zhejiang 315201, China

[§]Department of New Drug Development, School of Medicine, Inha University, Incheon 400-712, South Korea

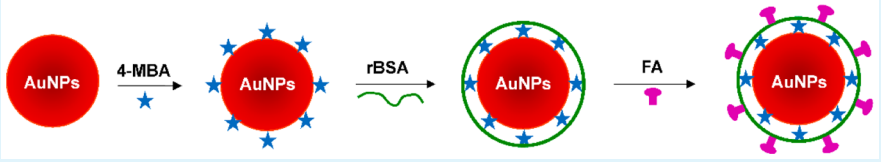

ABSTRACT: The detection of circulating tumor cells (CTCs) in the blood of cancer patients is crucial for early cancer diagnosis, cancer prognosis, evaluation of the treatment effect of chemotherapy drugs, and choice of cancer treatment options. In this study, we propose new surface-enhanced Raman scattering (SERS) nanoparticles for the direct detection of CTCs in the blood. Under the optimized experimental conditions, our SERS nanoparticles exhibit satisfying performances for the direct detection of cancer cells in the rabbit blood. A good linear relationship is obtained between the SERS intensity and the concentration of cancer cells in the range of 5−500 cells/mL (R^2 = 0.9935), which demonstrates that the SERS nanoparticles can be used for the quantitative analysis of cancer cells in the blood and the limit of detection is 5 cells/mL, which is lowest compared with the reported values. The SERS nanoparticles also have an excellent specificity for the detection of cancer cells in the rabbit blood. The above results reinforce that our SERS nanoparticles can be used for the direct detection of CTCs in the blood with excellent specificity and high sensitivity.

KEYWORDS: *surface-enhanced Raman scattering, circulating tumor cells, direct detection, blood, excellent specificity, high sensitivity*

1. INTRODUCTION

Circulating tumor cells (CTCs) fall from cancerous tumors into the bloodstream by a natural process and then circulate in the blood vessels. They may move to and remain in another tissue to grow and form a new metastasis, which may finally result in death of the cancer patients.[1,2] The liquid biopsy to longitudinally and repeatedly direct molecularly targeted therapy is one of the important applications of CTCs. In addition, the detection of CTCs in the blood of cancer patients is significant for early cancer diagnosis, cancer prognosis, evaluation of the treatment effect of chemotherapy drugs, and choice of cancer treatment options.[3−5] Although the detection of CTCs has important clinical and pathophysiological significance, the current techniques for detection of these rare cells are limited. In 1 mL of blood, there are around 5×10^9 erythrocytes and 1.0×10^7 leukocytes but only several CTCs.[4,6,7] Therefore, the detection of CTCs requires ultrasensitive methods.

Surface-enhanced Raman scattering (SERS) is one of the ultrasensitive methods that can be used for characterization at the molecular level.[8−10] Therefore, SERS offers a strong spectroscopy technology for the detection and identification of CTCs. Sha et al. developed magnetic beads for CTC capture and SERS tags (i.e., Nanoplex biotags) for CTC detection, whose calculated limit of detection (LOD) is ∼10 cells/mL.[11] Zhang et al. developed a simple method based on a new nitrocellulose membrane and SERS imaging technology for CTCs' sensitive detection and enumeration. A total of 34 out of 100 cancer cells spiked into 1 mL of blood can be captured and sorted by this method.[12] However, the majority of CTCs' SERS detection techniques require an initial enrichment step for capturing rare CTCs in whole blood, which makes the detection process more complicated.

In order to simplify the detection process, Wang et al. reported a new method using SERS technology for the direct detection of target CTCs in human peripheral blood. The LOD of this method ranges from 5 to 50 CTCs in 1 mL of blood.[13] However, there are still two problems that need to be solved: (1) the cost of the SERS nanoparticles, which mean nanoparticles with SERS activity, is very high because epidermal growth factor (EGF) is used as the targeted molecule; (2) the thick poly(ethylene glycol) (PEG) protection layer on the gold nanoparticle (AuNP) surface like "standing hair"[13] reduces the

Received: March 15, 2015
Accepted: April 15, 2015
Published: April 15, 2015

DOI: 10.1021/acsami.5b02276
ACS Appl. Mater. Interfaces 2015, 7, 9965−9971

Scheme 1. Schematic Illustration for the Design of SERS Nanoparticles

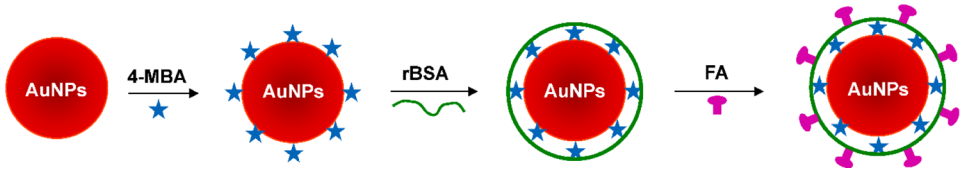

SERS signal because the Raman reporter molecule is inside the PEG protection layer.

Here, novel SERS nanoparticles for the direct detection of CTCs in the blood with excellent specificity and high sensitivity are proposed. As shown in Scheme 1, the AuNPs are encoded with a Raman reporter molecule, 4-mercaptobenzoic acid (4-MBA), and then functionalized with reductive bovine serum albumin (rBSA) to stabilize the 4-MBA-encoded AuNPs (AuNP−MBA) and decrease the nonspecific interaction with blood cells. A targeted ligand folic acid (FA) is then grated to the rBSA-stabilized AuNP−MBA (AuNP−MBA−rBSA) through the reaction between −COOH of FA and $-NH_2$ of rBSA to construct AuNP−MBA−rBSA−FA composite nanoparticles. The FA on the surface of AuNP−MBA−rBSA−FA nanoparticles can be recognized by CTCs of ovarian, brain, kidney, breast, lung, cervical, and nasopharyngeal cancer, which overexpress folate receptor alpha (FRα), and noncancer cells cannot. The key advantages include the following: (1) the cost is significantly decreased because FA is much cheaper than EGF; (2) the protection layer of rBSA, like "lying hair" (numerous −SH of rBSA broken up from disulfide bonds could form a Au−S bond on the AuNP surface), is much thinner than that of the reported PEG, like "standing hair", resulting in a stronger SERS signal.

2. MATERIALS AND METHODS

2.1. Materials. Gold(III) chloride trihydrate ($HAuCl_4{\cdot}3H_2O$) and sodium citrate dihydrate ($Na_3Ct{\cdot}2H_2O$) were obtained from Sinopharm Chemical Reagent Co. Ltd. (Shanghai, China). Bovine serum albumin (BSA), folic acid (FA), 4-mercaptobenzoic acid (4-MBA), sodium borohydride ($NaBH_4$), and 1-ethyl-3-[3-(dimethylamino)propyl]carbodiimide hydrochloride (EDC·HCl) were purchased from Aladdin Reagent Co. Ltd. (Shanghai, China). *N*-Hydroxysuccinimide (NHS) was obtained from Sigma-Aldrich. Trypsin−ethylenediaminetetraacetic acid (EDTA; 0.25%) and Dulbecco's modified Eagle medium (DMEM) were obtained from Gibco Life Technologies. A peripheral blood lymphocyte separation medium was obtained from Beijing Slolarbio Science and Technology Co. Ltd. (China). All other chemical reagents were of analytical grade and were used as received without further purification.

2.2. Preparation of AuNPs. AuNPs were prepared using a modified Turkevitch method, i.e., reduction of $HAuCl_4$ by Na_3Ct.[14,15] Briefly, a $HAuCl_4$ aqueous solution (5.0 mM, 10 mL) was mixed with pure water (30 mL). The diluted solution was then heated to boiling. After that, a Na_3Ct aqueous solution (10 mL, 1.0%) was rapidly charged to the boiling solution under vigorous stirring. After 3.0 min, the resulting AuNP dispersion, whose color changed from yellow to red, was cooled to room temperature. The obtained AuNPs were diluted 4-fold and kept in the fridge until further use.

2.3. Synthesis of SERS Nanoparticles. AuNPs were encoded with a Raman reporter molecule 4-MBA according to a modified approach.[16] Typically, 30.0 μL of 4-MBA in tetrahydrofuran with various concentrations (5.0−50 mM) was respectively added into 12.0 mL of the AuNP dispersion. The mixtures were allowed to react for 2.0 min under stirring at room temperature and then directly used for characterization of the SERS intensity.

The obtained 4-MBA-encoded AuNPs (AuNP−MBA) were subsequently functionalized with rBSA to stabilize AuNP−MBA and decrease the nonspecific interaction with blood cells. Briefly, 120 μL of a rBSA aqueous solution (reduced by $NaBH_4$) with different concentrations (0.05−1.0 mg/mL) was mixed with the AuNP−MBA solution (12.0 mL). The reaction was continued for 5.0 min at room temperature, and the samples were then directly used for characterization of the SERS intensity.

The targeted molecule FA was then grafted to the rBSA-stabilized AuNP−MBA nanoparticles (AuNP−MBA−rBSA) according to a modified approach through the reaction between −COOH of FA and $-NH_2$ of rBSA.[17,18] First, 40.0 mg of FA (90.4 μmol of −COOH), 32.0 mg of EDC (83.2 μmol), and 19.2 mg of NHS (83.2 μmol) were dissolved in 50 mL of phosphate-buffered saline (PBS; pH 7.4, 10 mM). The reaction was continued for 8.0 h at room temperature. After that, 0.1−2.0 mL of the above solution was respectively charged to 12.0 mL of the AuNP−MBA−rBSA dispersion, and the total volume was tuned to 14 mL with PBS. The mixtures were kept for 16 h at room temperature. The obtained FA-conjugated AuNP−MBA−rBSA nanoparticles (AuNP−MBA−rBSA−FA) were ultrafiltrated using Amicon Ultra-15 centrifugal filter units (Millipore, MWCO 3.0 kDa) (the supernatant was kept for UV−vis measurement), and the purified AuNP−MBA−rBSA−FA nanoparticles were dispersed in 2.0 mL of Milli-Q water for subsequent characterization of the SERS intensity and the detection of CTCs. The grafted content of FA on AuNP−MBA−rBSA nanoparticles was measured and calculated according to a previous mass balance method.[18]

Characterization of the nanoparticles by transmission electron microscopy (TEM), dynamic light scattering (DLS), and Raman spectra was conducted according to previous protocols.[18,19] Human breast cancer cell line MCF-7, human hepatocellular carcinoma cell line HepG2, and human cervical cancer cell line HeLa were cultured according to a previous protocol.[18]

2.4. Application of the SERS Nanoparticles for CTC Detection. The as-prepared SERS nanoparticles were used for CTC detection using a mixture of FRα-positive and FRα-negative cells to evaluate the specificity and sensitivity. Because cell lines with various expression levels of FRα may affect the detection results, the HepG2, HeLa, and MCF-7 cells with different expression levels of FRα were used in this study. HepG2 cells are FRα-negative cells,[20] and HeLa and MCF-7 cells are FRα-positive cells.[16,21−23] The FRα expression of the HeLa cells is much higher than that of the MCF-7 cells,[24] which should result in our SERS nanoparticles being more sensitive for the HeLa cells than the MCF-7 cells. In addition, the FRα expression is controlled by a gene, which cannot usually be changed during therapies. Therefore, the FRα expression should not be down-regulated or heterogeneous in tumors during therapies.[25,26]

For a study of the specificity, 200 μL of AuNP−MBA5−rBSA2−FA3 or AuNP−MBA5−rBSA2 (0.9 mg/mL) was added into 3.0 mL of cells in DMEM [2.3×10^6 HepG2 cells, 2×10^5 MCF-7 (or HeLa) cells, or 2.3×10^6 HepG2 cells plus 10^5 MCF-7 (or HeLa cells)] and then incubated for 30 min at 37 °C. The samples were centrifuged (400*g*, 5.0 min), washed thrice by PBS, and concentrated to 200 μL. After that, the SERS spectra of the samples were observed using a Raman instrument.

The same method was used to study the sensitivity. The only difference is that 100 μL of AuNP−MBA5−rBSA2−FA3 (0.9 mg/mL) was incubated with 3.0 mL of cells in DMEM containing 2.3×10^6 HepG2 cells and 10−10000 HeLa cells (or MCF-7 cells).

2.5. CTC Detection in the Rabbit Blood. All animal experiments were conducted in accordance with IACUC approved protocols.

DOI: 10.1021/acsami.5b02276
ACS Appl. Mater. Interfaces 2015, 7, 9965−9971

Table 1. Preparative Conditions and Results of the SERS Nanoparticles

nomenclature	$C_{4\text{-MBA}}$ (μM)	C_{rBSA} (μg/mL)	C_{FA} (μg/mL)	SERS intensity[a]	FCC (%)[b]
AuNP−MBA1	12.5			420	
AuNP−MBA2	25.0			1000	
AuNP−MBA3	50.0			2010	
AuNP−MBA4	75.0			1710	
AuNP−MBA5	125			3730	
AuNP−MBA5−rBSA1	125	10		1100	
AuNP−MBA5−rBSA2	125	5.0		3340	
AuNP−MBA5−rBSA3	125	2.0		3120	
AuNP−MBA5−rBSA4	125	1.0		2770	
AuNP−MBA5−rBSA5	125	0.5		4650	
AuNP−MBA5−rBSA2−FA1	125	5.0	114		
AuNP−MBA5−rBSA2−FA2	125	5.0	57.0		
AuNP−MBA5−rBSA2−FA3	125	5.0	28.5	64451	5.0 ± 2.2
AuNP−MBA5−rBSA2−FA4	125	5.0	11.4	53005	4.0 ± 2.1

[a]The determined SERS intensity of the nanoparticles at 1076 cm^{-1}. [b]Calculated from the weight ratio of conjugated FA to AuNP−MBA5−BSA2−FA nanoparticles. FCC: FA conjugation content.

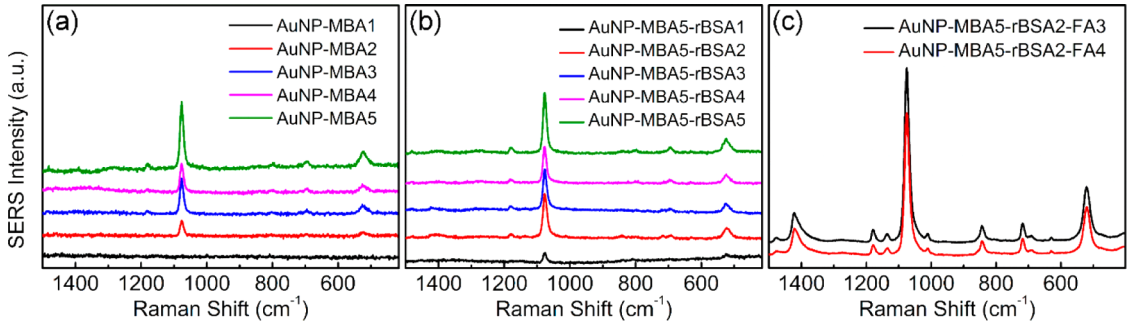

Figure 1. SERS spectra of the AuNP−MBA1−5 (a), AuNP−MBA5−rBSA1−5 (b), and AuNP−MBA5−rBSA2−FA3,4 nanoparticles (c). The excitation laser and data acquisition time are respectively set as 785 nm and 1.0 s.

Rabbit blood was collected into vacutainer tubes (containing lithium heparin) from the heart with vigorous shaking.

For a study of the sensitivity, 2.0 mL of PBS containing 10−10000 MCF-7 cells was mixed with the blood (2.0 mL) in centrifuge tubes. After that, the mixtures were respectively added into a peripheral blood lymphocyte separation medium (2.0 mL) and centrifuged at room temperature (400*g*, 25 min). The low-density cell layers containing white blood cells (WBCs; ~1.0×10^7) and MCF-7 cells were transferred to new tubes, rinsed twice by PBS, and dispersed in 3.0 mL of PBS. After that, 200 μL of AuNP−MBA5−rBSA2−FA3 (0.9 mg/mL) was mixed with the cells (3.0 mL) and incubated at 37 °C for 30 min. The samples were centrifuged (400*g*, 5.0 min), washed thrice by PBS, and concentrated to 200 μL. After that, the SERS spectra of the samples were observed using a Raman instrument.

The same approach was also used to study the specificity. The only difference is that 2.0 mL of the rabbit blood (~1.0×10^7 WBCs) without or with 10 MCF-7 cells was incubated with 200 μL of AuNP−MBA5−rBSA2 or AuNP−MBA5−rBSA2 (0.9 mg/mL).

3. RESULTS AND DISCUSSION

3.1. Preparation and Characterization of the SERS Nanoparticles. Preparation of the SERS nanoparticles is illustrated in Scheme 1. AuNPs prepared by a Turkevitch method[14,27] are encoded with a Raman reporter molecule 4-MBA via the Au−S bond. To stabilize the 4-MBA-encoded AuNPs (AuNP−MBA) and decrease the nonspecific interaction with blood cells, the AuNP−MBA nanoparticles are subsequently functionalized with rBSA, which has numerous −SH broken up from disulfide bonds of BSA and can bind to the AuNP surface via the Au−S bond like "lying hair". Therefore, the rBSA protection layer can be easily controlled to be very thin compared with the reported PEG protection layer like "standing hair".[13] The thinner protection layer could reduce the weakening effect of hydrophilic polymers on the SERS intensity of AuNPs. Furthermore, to increase the specificity of the rBSA-stabilized AuNP−MBA (AuNP−MBA−rBSA) toward CTCs among millions of healthy cells in the blood, the targeted molecule FA is grafted to AuNP−MBA−rBSA through the reaction between−COOH of FA and $-NH_2$ of rBSA.

The concentrations of 4-MBA, rBSA, and FA used for the preparation of AuNP−MBA−rBSA−FA are optimized according to the stability and SERS intensity of the nanoparticles. Table 1 shows the preparative conditions and results of the SERS nanoparticles, and Figure 1 shows the SERS spectra of the prepared nanoparticles. It is found that the SERS intensity of AuNP−MBA increases with an increase of the 4-MBA concentration from 12.5 to 125 μM (Figure 1a and Table 1). Because higher 4-MBA concentration results in poor stability of the nanoparticles, its optimal concentration is fixed at 125 μM in the following experiments.

As shown in Figure 1b and Table 1, the relative SERS intensity of AuNP−MBA−rBSA is very low (1100) when the rBSA concentration is 10 μg/mL but much stronger when the rBSA concentration is from 0.5 to 5.0 μg/mL (>2700). This result indicates that an overtight package of the SERS nanoparticles by hydrophilic polymers can reduce the SERS intensity. In addition, the stability and SERS intensity of AuNP−MBA−rBSA are comparable to each other when the

DOI: 10.1021/acsami.5b02276
ACS Appl. Mater. Interfaces 2015, 7, 9965−9971

rBSA concentration is in the range of 0.5−5.0 μg/mL (Figure 1b and Table 1). Because more FA could be conjugated onto the surface of AuNP−MBA−rBSA with more rBSA package, the rBSA concentration is fixed at 5.0 μg/mL as an optimal value in subsequent experiments.

The AuNP−MBA−rBSA−FA nanoparticles are not stable when the FA concentration is 114 or 57.0 μg/mL but very stable when the FA concentration is 28.5 or 11.4 μg/mL. The SERS intensities is also comparable to each other when the FA concentration is 28.5 or 11.4 μg/mL (Figure 1c and Table 1). Because the FA conjugation content (FCC) increases with an increase of the FA concentration, 28.5 μg/mL is chosen as the optimal FA concentration for the following study. The SERS intensity of AuNP−MBA−rBSA−FA is much stronger than that of AuNP−MBA−rBSA or AuNP−MBA, as shown in Table 1 because the AuNP−MBA−rBSA−FA solution was concentrated 7-fold by ultrafiltration before characterization of the SERS intensity and the detection of CTCs.

Parts a and b of Figure 2 show TEM images of AuNPs and AuNP−MBA−rBSA−FA, respectively. We can see that both

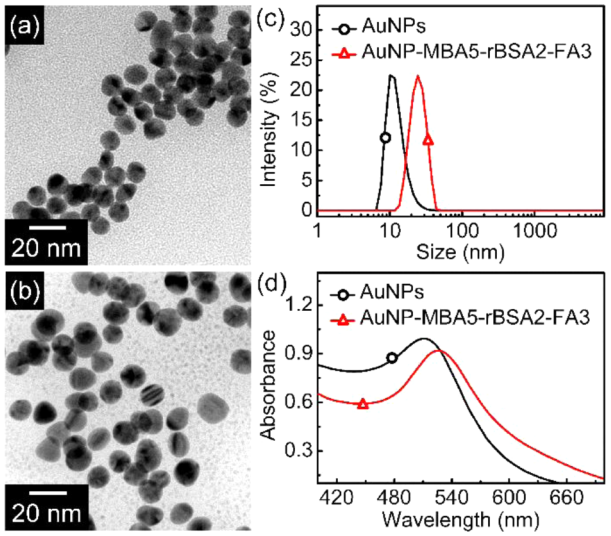

Figure 2. Characterization of the AuNPs (control) and SERS nanoparticles. TEM images of AuNPs (a) and AuNP−MBA5−rBSA2−FA3 (b). (c) Size distributions of AuNPs and AuNP−MBA5−rBSA2−FA3 in Milli-Q water at room temperature. (d) UV−vis spectra of AuNPs and AuNP−MBA5−rBSA2−FA3.

nanoparticles are well dispersed and the particle sizes are similar. Figure 2c shows the size distributions of AuNPs and AuNP−MBA5−rBSA2−FA3 in Milli-Q water measured by DLS. The hydrodynamic diameter is determined to be 17 nm for AuNPs and 21 nm for AuNP−MBA5−rBSA2−FA3. Both TEM and DLS results indicate that the rBSA protection layer is very thin, which is of great benefit to reducing its weakening effect on the SERS intensity. Figure 2d shows UV−vis spectra of AuNPs and AuNP−MBA5−rBSA2−FA3. The absorption peak is at 510 nm for AuNPs but shifts to 530 nm for AuNP−MBA5−rBSA2−FA3. The red shift of the surface plasmon band can be ascribed to the change of the refractive index surrounding the AuNPs.[28,29]

3.2. Specificity and Sensitivity of the CTC Detection System. It is well-known that CTCs are extremely rare in an extremely complex matrix. In 1 mL of blood, there are around 5 × 10^9 erythrocytes and 1.0 × 10^7 leukocytes but only several CTCs.[4] SERS spectroscopy is one of the ultrasensitive methods that can be used for characterization at the molecular level.[30−32] Therefore, SERS offers a strong spectroscopy technique for the detection and identification of CTCs. The main challenge of this method is to reduce the nonspecific binding of SERS nanoparticles to host blood cells, which outnumber CTCs by 5−6 orders of magnitude.[13] In this study, the specificity and sensitivity of our AuNP−MBA5−rBSA2−FA3-based CTC detection system are evaluated using HepG2 cells as negative cells and HeLa or MCF-7 cells as positive cells because HeLa and MCF-7 cells can overexpress FRα[16,21] but HepG2 cells cannot.[20]

Figure 3 shows the detection specificity of our AuNP−MBA5−rBSA2−FA3 nanoparticles for 10^5 HeLa (or MCF-7)

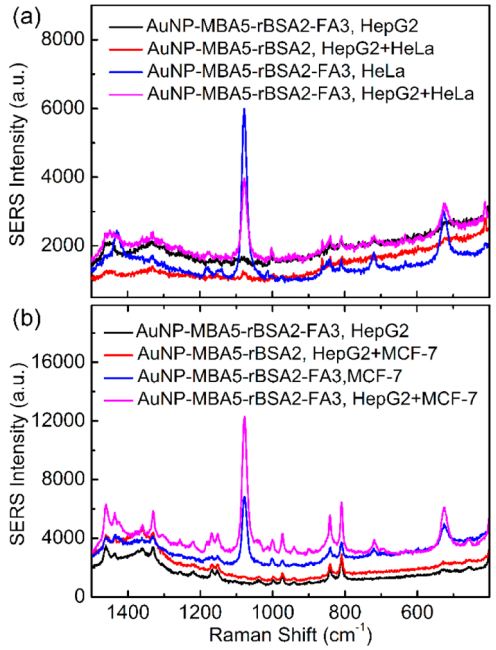

Figure 3. Detection specificity of our AuNP−MBA5−rBSA2−FA3 nanoparticles for 10^5 HeLa (or MCF-7) cells among 2.3 × 10^6 HepG2 cells. (a) SERS signals of the HepG2 cells, or HeLa cells, or HepG2 plus HeLa cells incubated with AuNP−MBA5−rBSA2−FA3 or AuNP−MBA5−rBSA2 nanoparticles. (b) SERS signals of the HepG2 cells, or MCF-7 cells, or HepG2 plus MCF-7 cells incubated with AuNP−MBA5−rBSA2−FA3 or AuNP−MBA5−rBSA2 nanoparticles.

cells in 2.3 × 10^6 HepG2 cells. Regarding the detection of HeLa cells in HepG2 cells, there is an obvious SERS peak at 1076 cm^{-1} for HeLa cells or HepG2 plus HeLa cells incubated with AuNP−MBA5−rBSA2−FA3, but no corresponding SERS peak is found for HepG2 cells incubated with AuNP−MBA5−rBSA2−FA3 or HepG2 plus HeLa cells incubated with AuNP−MBA5−rBSA2 (Figure 3a). A similar result is also obtained for the detection of MCF-7 cells in HepG2 cells (Figure 3b). These results indicate that our AuNP−MBA5−rBSA2−FA3 nanoparticles could be used for the detection of HeLa (or MCF-7) cells among HepG2 cells.

Figure 4 shows the detection sensitivity of our AuNP−MBA5−rBSA2−FA3 nanoparticles for HeLa (or MCF-7) cells in HepG2 cells. The SERS signals of 10−10000 HeLa cells in 2.3 × 10^6 HepG2 cells incubated with AuNP−MBA5−rBSA2−FA3 nanoparticles are shown in Figure 4a,b, and those of 10−500 MCF-7 cells in 2.3 × 10^6 HepG2 cells are shown in Figure

DOI: 10.1021/acsami.5b02276
ACS Appl. Mater. Interfaces 2015, 7, 9965−9971

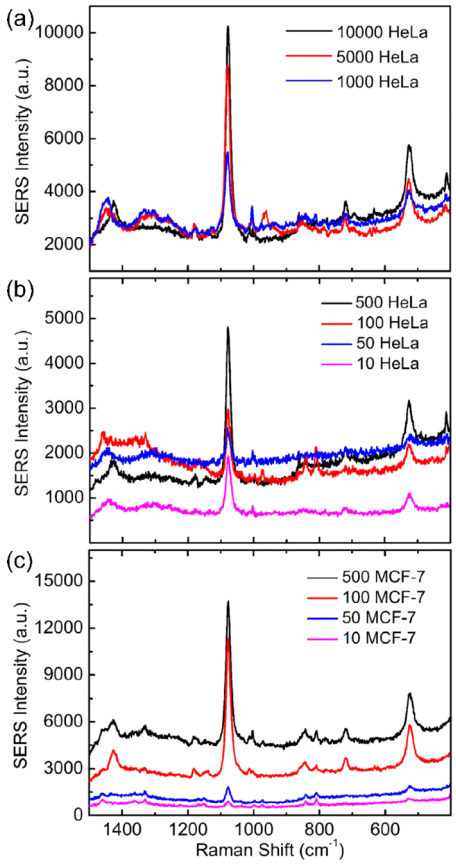

Figure 4. Detection sensitivity of our AuNP−MBA5−rBSA2−FA3 nanoparticles for HeLa (or MCF-7) cells among HepG2 cells. (a and b) SERS signals of 10−10000 HeLa cells among 2.3 × 10^6 HepG2 cells incubated with AuNP−MBA5−rBSA2−FA3 nanoparticles. (c) SERS signals of 10−500 MCF-7 cells among 2.3 × 10^6 HepG2 cells incubated with AuNP−MBA5−rBSA2−FA3 nanoparticles.

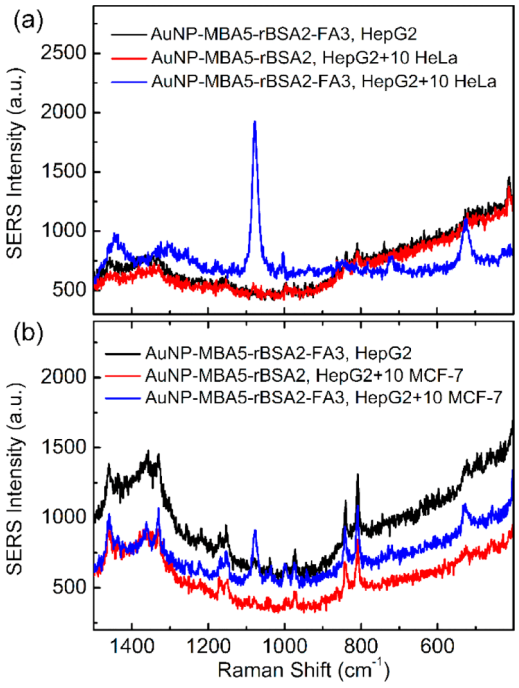

Figure 5. Detection specificity of our AuNP−MBA5−rBSA2−FA3 nanoparticles for 10 HeLa (or MCF-7) cells among 2.3 × 10^6 HepG2 cells. (a) SERS signals of the HepG2 cells or HepG2 plus 10 HeLa cells incubated with AuNP−MBA5−rBSA2−FA3 or AuNP−MBA5−rBSA2 nanoparticles. (b) SERS signals of the HepG2 cells or HepG2 plus 10 MCF-7 cells incubated with AuNP−MBA5−rBSA2−FA3 or AuNP−MBA5−rBSA2 nanoparticles.

4c. It can be seen that the SERS intensity increases with an increase in the amount of HeLa cells in the range of 10−10000 cells. A similar result is also obtained for MCF-7 cells. Because 10 HeLa (or MCF-7) cells among 2.3 × 10^6 HepG2 cells can also be found by our SERS nanoparticles, we can conclude that our AuNP−MBA5−rBSA2−FA3 nanoparticles are very sensitive for the detection of HeLa (or MCF-7) cells. In addition, from Figure 4b,c, we can see that our AuNP−MBA5−rBSA2−FA3 nanoparticles are more sensitive for HeLa cells than MCF-7 cells. That is because the FRα expression of HeLa cells is much higher than that of MCF-7 cells.[24]

The detection specificity of the AuNP−MBA5−rBSA2−FA3 nanoparticles for 10 HeLa (or MCF-7) cells among 2.3 × 10^6 HepG2 cells is further verified as shown in Figure 5. We can find an obvious SERS peak at 1076 cm^{-1} for 10 HeLa cells among 2.3 × 10^6 HepG2 cells incubated with AuNP−MBA5−rBSA2−FA3, but no corresponding SERS peak is found for 2.3 × 10^6 HepG2 cells incubated with AuNP−MBA5−rBSA2−FA3 or 10 HeLa cells among 2.3 × 10^6 HepG2 cells incubated with AuNP−MBA5−rBSA2 (Figure 5a). A similar result is also obtained for the detection of 10 MCF-7 cells among 2.3 × 10^6 HepG2 cells (Figure 5b). Therefore, we can conclude that our AuNP−MBA5−rBSA2−FA3 nanoparticles exhibit excellent specificity toward HeLa (or MCF-7) cells.

3.3. Detection of CTCs in the Rabbit Blood. The AuNP−MBA5−rBSA2−FA3 nanoparticles are also applied for the detection of cancer cells in the rabbit blood. Parts a and b of Figure 6 show the SERS signals of 2.0 mL of rabbit blood (∼1.0 × 10^7 WBCs) with 5−5000 MCF-7 cells/mL incubated with AuNP−MBA5−rBSA2−FA3 nanoparticles. It is found that the SERS intensity increases with an increase in the concentration of MCF-7 cells in the range of 5−5000 cells/mL. Figure 6c shows the plot of the SERS intensity as a function of the concentration of MCF-7 cells spiked into the rabbit blood. The inset plot shows the SERS intensity versus different concentration of MCF-7 cells in the range of 5−500 cells/mL (R^2 = 0.9935). The good linear relationship demonstrates that the proposed SERS nanoparticles could be used to quantitatively analyze the cancer cells, and the LOD is 5 cells/mL, which is lowest compared to the reported values.[11,13] The LOD is ∼10 cells/mL for the SERS tags (i.e., Nanoplex biotags) developed by Sha et al.[11] and in the range of 5−50 cells/mL for the SERS nanoparticles developed by Wang et al.[13]

The detection specificity of the AuNP−MBA5−rBSA2−FA3 nanoparticles for 10 MCF-7 cells in 2.0 mL of rabbit blood is also verified. Figure 7 shows the SERS signals of 2.0 mL of rabbit blood (∼1.0 × 10^7 WBCs) without or with 10 MCF-7 cells incubated with AuNP−MBA5−rBSA2−FA3 or AuNP−MBA5−rBSA2 nanoparticles. The SERS peak at 1076 cm^{-1} is obvious for 2.0 mL of rabbit blood with 10 MCF-7 cells incubated with AuNP−MBA5−rBSA2−FA3, but no corresponding SERS peak is found for 2.0 mL of rabbit blood with 10 MCF-7 cells incubated with AuNP−MBA5−rBSA2 or 2.0 mL of rabbit blood without MCF-7 cells incubated with AuNP−MBA5−rBSA2−FA3. Therefore, we can conclude that

DOI: 10.1021/acsami.5b02276
ACS Appl. Mater. Interfaces 2015, 7, 9965−9971

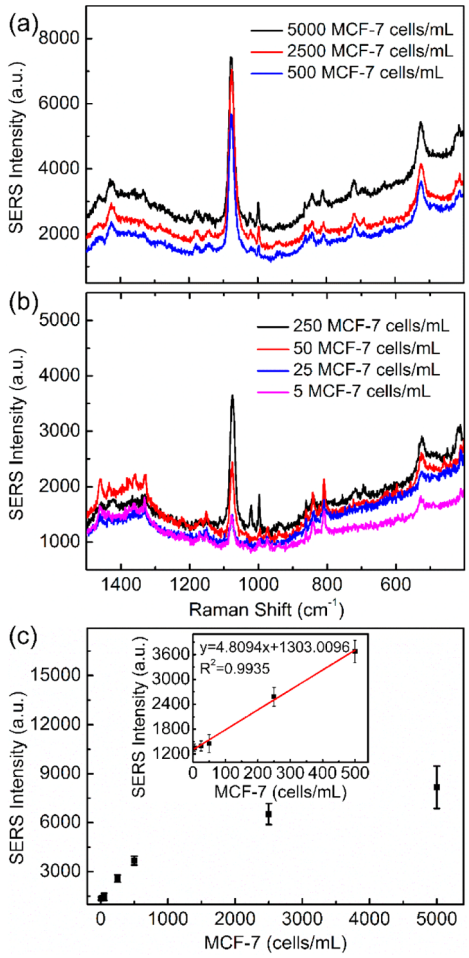

Figure 6. Detection sensitivity of the AuNP−MBA5−rBSA2−FA3 nanoparticles for MCF-7 cells in the rabbit blood. (a and b) SERS signals of 2.0 mL of rabbit blood (~1.0 × 10^7 WBCs) with 5−5000 MCF-7 cells/mL incubated with AuNP−MBA5−rBSA2−FA3 nanoparticles. (c) Plot of the SERS intensity as a function of the concentration of MCF-7 cells spiked into the rabbit blood.

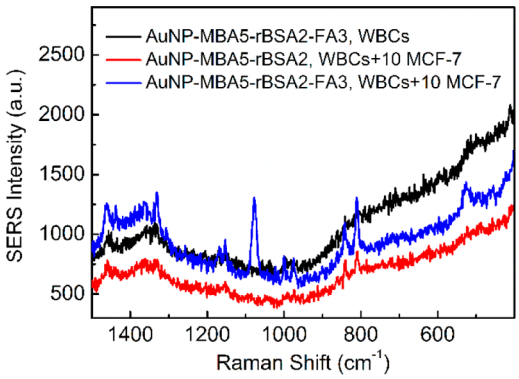

Figure 7. Detection specificity of the AuNP−MBA5−rBSA2−FA3 nanoparticles for MCF-7 cells in the rabbit blood. SERS signals of 2.0 mL of rabbit blood (~1.0 × 10^7 WBCs) without or with 10 MCF-7 cells incubated with AuNP−MBA5−rBSA2−FA3 or AuNP−MBA5−rBSA2 nanoparticles.

AuNP−MBA5−rBSA2−FA3 nanoparticles are highly specific for the detection of cancer cells in the rabbit blood.

The above results reinforce that our AuNP−MBA5−rBSA2−FA3 nanoparticles are improved SERS nanoparticles and could be applied to directly detect CTCs in the blood with excellent specificity and high sensitivity.

The SERS technology may provide molecular characterization of CTCs at the single cell level because it is ultrasensitive down to the single molecular level.[8−10]

In this study, rabbit blood was used instead of human blood for the following reasons: (1) The rabbit blood is more easily obtained. (2) The detection effect should be similar because several cancer cells (i.e., ovarian, brain, kidney, breast, lung, cervical, and nasopharyngeal cancer cells) can overexpress the FRα and noncancer cells in human blood and rabbit blood cannot.[33,34] Although human monocytes and other noncancer cells may express FRα slightly, its expressed amount should be much lower than that of the above-mentioned cancer cells.[35] Therefore, the results obtained from the rabbit blood indicate that our SERS nanoparticles could be used for the detection of CTCs in the human blood. We will cooperate with some hospitals to obtain the human blood in the next study.

4. CONCLUSIONS

In summary, we have developed new SERS nanoparticles for the direct detection of CTCs in the blood with excellent specificity and high sensitivity. AuNPs are encoded with a Raman reporter molecule 4-MBA, functionalized with hydrophilic polymer rBSA, and targeted by molecule FA to construct AuNP−MBA−rBSA−FA composite nanoparticles. According to the stability and SERS intensity of the AuNP−MBA−rBSA−FA nanoparticles, the concentrations of 4-MBA, rBSA, and FA are optimized to be 125 μM, 5.0 μg/mL, and 28.5 μg/mL, respectively. The TEM and DLS results indicate that the well-dispersed spherical AuNP−MBA−rBSA−FA has a very thin rBSA protection layer, which is of great benefit to reducing its weakening effect on the SERS intensity. Under the optimized experimental conditions, our AuNP−MBA−rBSA−FA nanoparticles exhibit satisfying performances for the direct detection of cancer cells in the rabbit blood. There is a good linear relationship (R^2 = 0.9935) between the SERS intensity and the concentration of cancer cells in the range of 5−500 cells/mL. The strong linear relationship indicates that our AuNP−MBA−rBSA−FA nanoparticles can be used for the quantitative analysis of CTCs, and the LOD is 5 cells/mL, which is lowest compared with the reported values. In addition, the AuNP−MBA5−rBSA2−FA3 nanoparticles have an excellent specificity for the detection of cancer cells in the rabbit blood.

AUTHOR INFORMATION

Corresponding Authors

*E-mail: shenzheyu@nimte.ac.cn. Tel: +86 574 87617278. Fax: +86-57486685163.

*E-mail: aiguo@nimte.ac.cn. Tel: +86 574 86685039. Fax: +86-57486685163.

Notes

The authors declare no competing financial interest.

ACKNOWLEDGMENTS

This work is financially supported by National Natural Science Foundation of China (Grants 51203175, 51411140243, and 61171033), Zhejiang Provincial Natural Science Foundation of China (Grant LQ13E030004), Hundred Talents Program of Chinese Academy of Sciences (2010-735), and National Research Foundation of Korea (NRF-2014K2A2A2000720).

DOI: 10.1021/acsami.5b02276
ACS Appl. Mater. Interfaces 2015, 7, 9965−9971

REFERENCES

(1) Webb, J. A.; Rizia, B. Emerging Advances in Nanomedicine with Engineered Gold Nanostructures. *Nanoscale* **2014**, *6*, 2502−2530.

(2) Adams, A. A.; Okagbare, P. I.; Feng, J.; Hupert, M. L.; Patterson, D.; Gottert, J.; McCarley, R. L.; Nikitopoulos, D.; Murphy, M. C.; Soper, S. A. Highly Efficient Circulating Tumor Cell Isolation from Whole Blood and Label-Free Enumeration Using Polymer-Based Microfluidics with an Integrated Conductivity Sensor. *J. Am. Chem. Soc.* **2008**, *130*, 8633−8641.

(3) Wang, S. Q.; Wan, Y.; Liu, Y. L. Effects of Nanopillar Array Diameter and Spacing on Cancer Cell Capture and Cell Behaviors. *Nanoscale* **2014**, *6*, 12482−12489.

(4) Paterlini, B. P.; Benali, N. L. Circulating Tumor Cells (CTC) Detection: Clinical Impact and Future Directions. *Cancer Lett.* **2007**, *253*, 180−204.

(5) Wen, C. Y.; Wu, L. L.; Zhang, Z. L.; Liu, Y. L.; Wei, S. Z.; Hu, J.; Tang, M.; Sun, E. Z.; Gong, Y. P.; Yu, J.; Pang, D. W. Quick-Response Magnetic Nanospheres for Rapid, Efficient Capture and Sensitive Detection of Circulating Tumor Cells. *ACS Nano* **2013**, *8*, 941−949.

(6) Chen, W.; Weng, S.; Zhang, F.; Allen, S.; Li, X.; Bao, L.; Lam, R. H. W.; Macoska, J. A.; Merajver, S. D.; Fu, Q. Nanoroughened Surfaces for Efficient Capture of Circulating Tumor Cells without Using Capture Antibodies. *ACS Nano* **2012**, *7*, 566−575.

(7) Cristofanilli, M.; Budd, G. T.; Ellis, M. J.; Stopeck, A.; Matera, J.; Miller, M. C.; Reuben, J. M.; Doyle, G. V.; Allard, W. J.; Terstappen, L. W. M. M.; Hayes, D. F. Circulating Tumor Cells, Disease Progression, and Survival in Metastatic Breast Cancer. *New Engl. J. Med.* **2004**, *351*, 781−791.

(8) Jin, X. L.; Li, H. Y.; Wang, S. S.; Kong, N.; Xu, H.; Fu, Q. H.; Gu, H. C.; Ye, J. Multifunctional Superparamagnetic Nanoshells: Combining Two-Photon Luminescence Imaging, Surface-Enhanced Raman Scattering and Magnetic Separation. *Nanoscale* **2014**, *6*, 14360−14370.

(9) Chen, L. X.; Fu, X. L.; Li, J. H. Ultrasensitive Surface-Enhanced Raman Scattering Detection of Trypsin Based on Anti-aggregation of 4-Mercaptopyridine-Functionalized Silver Nanoparticles: an Optical Sensing Platform Toward Proteases. *Nanoscale* **2013**, *5*, 5905−5911.

(10) Fan, X.; Lee, Y. H.; Pedireddy, S.; Zhang, Q.; Liu, T. X.; Ling, X. Y. Graphene Oxide and Shape-Controlled Silver Nanoparticle Hybrids for Ultrasensitive Single-Particle Surface-Enhanced Raman Scattering (SERS) Sensing. *Nanoscale* **2014**, *6*, 4843−4851.

(11) Sha, M. Y.; Xu, H.; Natan, M. J.; Cromer, R. Surface-Enhanced Raman Scattering Tags for Rapid and Homogeneous Detection of Circulating Tumor Cells in the Presence of Human Whole Blood. *J. Am. Chem. Soc.* **2008**, *130*, 17214−17215.

(12) Zhang, P.; Zhang, R.; Gao, M.; Zhang, X. Novel Nitrocellulose Membrane Substrate for Efficient Analysis of Circulating Tumor Cells Coupled with Surface-Enhanced Raman Scattering Imaging. *ACS Appl. Mater. Interfaces* **2013**, *6*, 370−376.

(13) Wang, X.; Qian, X. M.; Beitler, J. J.; Chen, Z. G.; Khuri, F. R.; Lewis, M. M.; Shin, H. J. C.; Nie, S. M.; Shin, D. M. Detection of Circulating Tumor Cells in Human Peripheral Blood Using Surface-Enhanced Raman Scattering Nanoparticles. *Cancer Res.* **2011**, *71*, 1526−1532.

(14) Turkevich, J.; Stevenson, P. C.; Hillier, J. A Study of the Nucleation and Growth Processes in the Synthesis of Colloidal Gold. *Discuss. Faraday Soc.* **1951**, *11*, 55−75.

(15) Li, Y. L.; Leng, Y. M.; Zhang, Y. J.; Li, T. H.; Shen, Z. Y.; Wu, A. G. A New Simple and Reliable Hg^{2+} Detection System Based on Anti-aggregation of Unmodified Gold Nanoparticles in the Presence of *o*-phenylenediamine. *Sens. Actuators, B* **2014**, *200*, 140−146.

(16) Wei, L. J.; Jin, B.; Dai, S. Polymer Microbead-Based Surface Enhanced Raman Scattering Immunoassays. *J. Phys. Chem. C* **2012**, *116*, 17174−17181.

(17) Shen, Z.; Li, Y.; Kohama, K.; Oneill, B.; Bi, J. Improved Drug Targeting of Cancer Cells by Utilizing Actively Targetable Folic Acid-Conjugated Albumin Nanospheres. *Pharmacol. Res.* **2011**, *63*, 51−58.

(18) Ma, X. H.; Gong, A.; Xiang, L. C.; Chen, T. X.; Gao, Y. X.; Liang, X. J.; Shen, Z. Y.; Wu, A. G. Biocompatible Composite Nanoparticles with Large Longitudinal Relaxivity for Targeted Imaging and Early Diagnosis of Cancer. *J. Mater. Chem. B* **2013**, *1*, 3419−3428.

(19) Zhao, X.; Hosmane, N. S.; Wu, A. *ortho*-Phenylenediamine: An Effective Spacer to Build Highly Magnetic Fe_3O_4/Au Nanocomposites. *ChemPhysChem* **2012**, *13*, 4142−4147.

(20) Nour, A. M. A.; Ringot, D.; Gueant, J. L.; Chango, A. Folate Receptor and Human Reduced Folate Carrier Expression in HepG2 Cell Line Exposed to Fumonisin B-1 and Folate Deficiency. *Carcinogenesis* **2007**, *28*, 2291−2297.

(21) Geng, J.; Li, K.; Ding, D.; Zhang, X.; Qin, W.; Liu, J.; Tang, B. Z.; Liu, B. Lipid-PEG-Folate Encapsulated Nanoparticles with Aggregation Induced Emission Characteristics: Cellular Uptake Mechanism and Two-Photon Fluorescence Imaging. *Small* **2012**, *8*, 3655−3663.

(22) Das, M.; Datir, S. R.; Singh, R. P.; Jain, S. Augmented Anticancer Activity of a Targeted, Intracellularly Activatable, Theranostic Nanomedicine Based on Fluorescent and Radiolabeled, Methotrexate−Folic Acid−Multiwalled Carbon Nanotube Conjugate. *Mol. Pharmaceutics* **2013**, *10*, 2543−2557.

(23) O'Shannessy, D. J.; Somers, E. B.; Maltzman, J.; Smale, R.; Fu, Y. S. Folate Receptor Alpha (FRA) Expression in Breast Cancer: Identification of a New Molecular Subtype and Association with Triple Negative Disease. *SpringerPlus* **2012**, *1*, 22.

(24) Feng, D.; Song, Y.; Shi, W.; Li, X.; Ma, H. Distinguishing Folate-Receptor-Positive Cells from Folate-Receptor-Negative Cells Using a Fluorescence Off−On Nanoprobe. *Anal. Chem.* **2013**, *85*, 6530−6535.

(25) Crane, L. M. A.; Arts, H. J. G.; Oosten, M.; Low, P. S.; Zee, A. G. J.; Dam, G. M.; Bart, J. The effect of chemotherapy on expression of folate receptor-alpha in ovarian cancer. *Cell. Oncol.* **2012**, *35*, 9−18.

(26) Despierre, E.; Lambrechts, S.; Leunen, K.; Berteloot, P.; Neven, P.; Amant, F.; O'Shannessy, D. J.; Somers, E. B.; Vergote, I. Folate receptor alpha (FRA) expression remains unchanged in epithelial ovarian and endometrial cancer after chemotherapy. *Gynecol. Oncol.* **2013**, *130*, 192−199.

(27) Llevot, A.; Astruc, D. Applications of Vectorized Gold Nanoparticles to the Diagnosis and Therapy of Cancer. *Chem. Soc. Rev.* **2012**, *41*, 242−257.

(28) Yortyot, S. N.; Wansadaj, J.; Siriporn, S.; Rungkarn, S.; Wansika, K. Visual Detection of White Spot Syndrome Virus Using DNA-Functionalized Gold Nanoparticles as Probes Combined With Loop-Mediated Isothermal Amplification. *Mol. Cell. Probes* **2013**, *27*, 71−79.

(29) Jie, Y.; Akram, H.; Christeen, G.; Pierre, B.; Shan, Z. Ordered Gold Nanoparticle Arrays on Glass and Their Characterization. *J. Colloid Interface Sci.* **2013**, *410*, 1−10.

(30) Qian, X.; Peng, X. H.; Ansari, D. O.; Yin-Goen, Q.; Chen, G. Z.; Shin, D. M.; Yang, L.; Young, A. N.; Wang, M. D.; Nie, S. M. In Vivo Tumor Targeting and Spectroscopic Detection with Surface-Enhanced Raman Nanoparticle Tags. *Nat. Biotechnol.* **2008**, *26*, 83−90.

(31) Moore, B. D.; Stevenson, L.; Watt, A.; Flitsch, S.; Turner, N. J.; Cassidy, C.; Graham, D. Rapid and Ultra-sensitive Determination of Enzyme Activities Using Surface-Enhanced Resonance Raman Scattering. *Nat. Biotechnol.* **2004**, *22*, 1133−1138.

(32) Tian, J. H.; Liu, B.; Li, X. L.; Yang, Z. L.; Ren, B.; Wu, S. T.; Tao, N. J.; Tian, Z. Q. Study of Molecular Junctions with a Combined Surface-Enhanced Raman and Mechanically Controllable Break Junction Method. *J. Am. Chem. Soc.* **2006**, *128*, 14748−14749.

(33) Noble, C. O.; Kirpotin, D. B.; Hayes, M. E.; Mamot, C.; Hong, K.; Park, J. W.; Benz, C. C.; Marks, J. D.; Drummond, D. C. Development of Ligand-Targeted Liposomes for Cancer Therapy. *Expert Opin. Ther. Targets* **2004**, *8*, 335−353.

(34) Kamen, B. A.; Smith, A. K. A Review of Folate Receptor Alpha Cycling and 5-Methyltetrahydrofolate Accumulation with an Emphasis on Cell Models in Vitro. *Adv. Drug Delivery Rev.* **2004**, *56*, 1085−1097.

(35) Hala, E.; Manohar, R. Distribution, Functionality and Gene Regulation of Folate Receptor Isoforms: Implications in Targeted Therapy. *Adv. Drug Delivery Rev.* **2004**, *56*, 1067−1084.

DOI: 10.1021/acsami.5b02276
ACS Appl. Mater. Interfaces 2015, 7, 9965−9971